

1 **Population pharmacokinetic modeling of tribendimidine metabolites in *Opisthorchis***  
2 ***viverrini*-infected adults**

3 Fiona Vanobberghen,<sup>a,b</sup># Melissa Penny,<sup>a,b</sup> Urs Duthaler,<sup>a,b</sup>† Peter Odermatt,<sup>a,b</sup> Somphou  
4 Sayasone,<sup>c</sup> Jennifer Keiser,<sup>a,b</sup>\* Joel Tarning<sup>d,e</sup>\*

5

6 <sup>a</sup>Swiss Tropical & Public Health Institute, Basel, Switzerland

7 <sup>b</sup>University of Basel, Basel, Switzerland

8 <sup>c</sup>National Institute of Public Health, Vientiane, Lao PDR

9 <sup>d</sup>Mahidol-Oxford Tropical Medicine Research Unit, Faculty of Tropical Medicine, Mahidol  
10 University, Bangkok, Thailand

11 <sup>e</sup>Centre for Tropical Medicine and Global Health, Nuffield Department of Medicine,  
12 University of Oxford, Oxford, UK

13

14 **Running head:** Pharmacokinetic modeling of tribendimidine

15 **# Correspondence to:** Fiona Vanobberghen, Swiss Tropical and Public Health Institute,  
16 Socinstrasse 57, 4051, Basel, Switzerland

17 **† Present address:** Department of Biomedicine, University Hospital Basel, Hebelstrasse 20,  
18 4031 Basel, Switzerland

19 \* Contributed equally

20 **Word count:** 3446

21 Tables 3, figures 4

22 **Keywords:** tribendimidine, population pharmacokinetics, *Opisthorchis viverrini*, Laos

23

24   **ABSTRACT**

25   There is pressing need for alternative treatments against the liver fluke *Opisthorchis viverrini*.  
26   Oral tribendimidine is a promising candidate, but its population pharmacokinetic properties  
27   are unknown.

28

29   Two phase IIa trials were conducted in Laos in *O. viverrini*-infected adults receiving single oral  
30   doses of 25-600 mg tribendimidine, administered as different formulations in each study  
31   (study 1 used 200 mg tablets; study 2 used 50 mg tablets). Venous whole-blood, plasma and  
32   capillary dried blood spots were sampled frequently from 68 adults and concentrations of  
33   tribendimidine metabolites dADT (deacetylated amidantel) and adADT (acetylated dADT)  
34   were measured. Population pharmacokinetics were assessed using nonlinear mixed-effects  
35   modeling. The relationship between drug exposure and cure (assessed 21 days post-  
36   treatment) was evaluated using univariable logistic regression.

37

38   A six-transit compartment absorption model with a one-disposition compartment for each  
39   metabolite described the data well. Compared to the 50 mg formulation (study 2), the 200  
40   mg formulation (study 1) had 40.1% higher mean transit absorption time, 113% higher dADT  
41   volume of distribution, and 364% higher adADT volume of distribution. Each ten year  
42   increase in age was associated with 12.7% lower dADT clearance and 21.2% lower adADT  
43   clearance. Highest cure rates ( $\geq 55\%$ ) were observed with doses  $\geq 100$  mg. Higher dADT, but  
44   not adADT, peak concentrations and exposures were associated with cure ( $p=0.004$  and  
45   0.003, respectively).

46

47 For the first time population pharmacokinetics of tribendimidine has been described. Known  
48 differences in the 200 mg versus 50 mg formulations were captured by covariate modeling.  
49 Further studies are needed to validate the structural model and confirm covariate  
50 relationships.

51

## 52 INTRODUCTION

53 Helminthic infections present a challenging public health problem, with over 40 million  
54 people worldwide infected with food-borne trematodiasis (1). The burden is  
55 disproportionately higher in resource-limited settings (2). In south-east Asia, an estimated 8-  
56 10 million people are infected with the liver fluke *Opisthorchis viverrini* (1). While most  
57 infections are symptom-free, severe manifestations may occur in the bile duct or gall  
58 bladder (cholangitis, cholecystitis, cholelithiasis), and *O. viverrini* is a risk factor for the bile  
59 duct cancer cholangiocarcinoma (3). Praziquantel is the only drug currently available,  
60 therefore there is a pressing need to identify alternatives (4, 5). Efforts are being made to  
61 develop new or repurpose old drugs for helminthic treatment (2, 6).

62  
63 Oral tribendimidine was first synthesized in China in the 1980s and has been marketed there  
64 since 2004 against hookworms, *Ascaris lumbricoides* and *Enterobius vermicularis* (7). It is a  
65 promising candidate for the treatment of *O. viverrini* infection (8). In an open label  
66 randomized phase II trial, tribendimidine had high efficacy against *O. viverrini*, with no  
67 difference compared to praziquantel (9), and in a subsequent pair of phase IIa dose-finding  
68 trials, excellent efficacy at tribendimidine doses of 100 mg and above was observed, with the  
69 highest efficacy observed at 400 mg (cure rate 91.5% and egg reduction rate 99.8%; Sayasone  
70 *et al*, manuscript under review). Tribendimidine is highly unstable and degrades  
71 spontaneously into deacetylated amidantel (dADT) and terephthalaldehyde (TPAL) in water  
72 without the involvement of metabolic enzymes (10). This process is accelerated at low pH  
73 like in the gastrointestinal gut, therefore the tablets are commercialized as an enteric-coated  
74 formulation. dADT is partially converted to acetylated dADT (adADT), with 35%-53%  
75 excreted unchanged in urine (10, 11), and TPAL metabolizes completely into terephthalic acid

76 (TPAC) (10). TPAL and TPAC are pharmacologically inactive metabolites, whereas dADT is  
77 highly active and adADT has marginal or no anthelmintic activity (12).  
78  
79 Knowledge of drug pharmacokinetic (PK) properties is essential to inform dosing, and may  
80 inform drivers of cure, yet to date limited data are available to inform the drug exposure to  
81 oral doses of tribendimidine. Small studies in China (each  $\leq 30$  participants) have described  
82 the basic PK properties in healthy volunteers ((10, 11, 13–15) in Chinese; (10, 11, 14, 15) are  
83 summarized in (8)). In the phase IIa dose finding trials mentioned above, we investigated the  
84 model-independent PK properties among persons infected with *O. viverrini* (Duthaler *et al*,  
85 manuscript under review). However, the population PK properties remain unknown, which  
86 are crucial in order to assess influential covariates and to develop a rational framework for  
87 future clinical trial simulations. The aim of this study was to determine the population PK  
88 properties of tribendimidine in persons infected with *O. viverrini*, and to investigate the  
89 relationship with cure.

90

## 91 **MATERIALS AND METHODS**

### 92 **Study design and ethical considerations**

93 Two phase IIa open-label, randomized, ascending dose finding trials were conducted in Laos,  
94 in November 2012 and October 2013, with similar methodology. Details on the trials are  
95 presented elsewhere (Sayasone *et al*, manuscript under review). Eligible patients identified  
96 through clinical examination and interviews were those who did not suffer from major  
97 systemic or chronic illness, psychiatric disorders, and were not pregnant. Stool samples  
98 were taken prior to treatment and 21 days later, to estimate the egg burden before and  
99 after treatment in order to quantify the pharmacodynamic effects of tribendimidine against

100 *O. viverrini*. At each of these time-points, two stool samples were collected on different days  
101 within a maximum of three days and two Kato-Katz thick smears (41.7 mg) were prepared  
102 from each stool (Sayasone *et al*, manuscript under review). In the framework of these trials,  
103 *O. viverrini*-positive patients were admitted to Champasack Provincial Hospital, Pakse for 24  
104 hours for participation in a PK study. The PK study, including non-compartmental PK results,  
105 is reported in full elsewhere (Duthaler *et al*, manuscript under review) and details are given  
106 below.

107  
108 The studies were approved by the Ethics Committee of the Ministry of Health, Vientiane,  
109 Laos (reference 009/NECHR), the Ethical Committee of the Canton of Basel-Stadt and Basel-  
110 Land, Basel, Switzerland (EKBB; reference 375/11), and the Liverpool School of Tropical  
111 Medicine Research Ethics Committee, UK (reference 12.02RS). The study was registered on  
112 the ISRCTN registry (ISRCTN96948551). Informed consent written in Lao language was read  
113 and explained by a researcher to each participant and all participants provided written  
114 informed consent.

#### 115 116 **Treatment and blood sampling**

117 Participants received single oral doses of 200, 400 and 600 mg tribendimidine (using 200 mg  
118 enteric-coated tablets) in the first trial, and doses of 25, 50, 100 and 200 mg (using 50 mg  
119 enteric-coated tablets) in the second trial (all tablets produced by Shandong Xinghua  
120 Pharmaceutical Corporation, China). Of note, different absorption properties of the two  
121 formulations were hypothesized since they have been observed previously (Duthaler *et al*,  
122 manuscript under review).

Venous blood sampling was performed at approximately 0, 1, 2, 3, 4, 4.5, 5, 6, 8, 10, 24 hours post-dose to assess both whole-blood and plasma drug concentrations. As detailed elsewhere (Duthaler *et al*, manuscript under review), 4mL venous blood was collected; 1 ml was transferred in a labeled tube, within 30 minutes post sampling, and the remaining sample was centrifuged to produce plasma. The samples stored at -80° C. Capillary blood samples (0.1 mL) were taken by fingertip puncture at approximately 0, 2, 4, 5, 8, 24 hours post-dose, to validate a novel dried blood spot (DBS) method for drug quantification (16). Four drops of blood were transferred onto filter paper and dried for approximately one hour. Plasma and DBS measurements were performed in both studies while whole-blood measurements were performed in the first study only.

#### **Drug measurements**

The active metabolites dADT and adADT were quantified in venous whole-blood, plasma and capillary blood on filter paper using a validated liquid chromatography tandem mass spectrometry method (16). The lower limit of quantification (LLOQ) was 1 ng/mL for whole-blood and plasma, and 10 ng/mL for DBS in the first study (16); in the second study, the LLOQ for DBS was reduced to 1 ng/ml since the doses were up to 10 times lower. The within-day and between-day accuracy and precision at low, mid, and high quality control levels were below 15% (LLOQ: 20%) throughout clinical samples analysis (Duthaler *et al*, manuscript under review).

#### **Pharmacokinetic and statistical analyses**

Data were processed using Stata version 12 (StataCorp. 2011. *Stata Statistical Software: Release 12*. College Station, TX: StataCorp LP). Graphics were created using R (version 3.0.2; The R Foundation for Statistical Computing).

Whole-blood, plasma and DBS concentrations were pooled across both studies, and molar units of dADT and adADT were transformed into their natural logarithms and modeled simultaneously using nonlinear mixed-effects modeling. Estimations and simulations were performed using NONMEM 7.1.2 (17) with Piraña 2.8.2 (18) and Perl-speaks-NONMEM (PsN) (19). The first-order conditional estimation method with interactions or the Laplacian estimation method was used throughout the modeling. A fixed renal clearance of dADT of 35% was assumed since no urine data were available (10); the remaining 65% was assumed to be completely metabolized into adADT. One-compartment and two-compartment disposition models were considered for each metabolite, using a first-order absorption model. Different absorption models were then evaluated using the best performing disposition model, i.e. first-order absorption and a more flexible transit-absorption model (stepwise addition of transit compartments with transit rate constant set equal to the absorption rate constant). Relative bioavailability (F), fixed to unity for the population but allowing for inter-individual variability on that parameter, was evaluated. Inter-individual random variability in all parameters was modeled exponentially using  $\theta_i = \theta_{TV} \times \exp(\eta_{i,\theta})$  where  $\theta_i$  is the individually-estimated parameter value for the  $i^{th}$  patient,  $\theta_{TV}$  is the typical parameter value for the modeled population, and  $\eta_{i,\theta}$  is the inter-individual random variability, assumed to be normally-distributed with zero mean and variance  $\omega^2$ . Potential correlations between the clearance and volume parameters for both metabolites were evaluated with a full variance-covariance matrix. The residual unexplained variability was



170 modeled as a separate additive error for each metabolite on the log-transformed  
171 concentrations, which is essentially equivalent to an exponential residual error on the  
172 arithmetic scale. A proportional transformation factor for plasma, DBS and whole-blood  
173 (without inter-individual variability) was evaluated to allow for systematic differences  
174 between sampling matrices (20). Values below the limit of quantification were omitted  
175 initially, but subsequently evaluated as censored observations using the M3 method (21).  
176  
177 Body weight was evaluated as an allometric function on all clearance and volume  
178 parameters (i.e. exponent of 0.75 and 1 for clearance and volume parameters, respectively  
179 (22)). Other biologically-plausible covariates (age, sex, creatinine clearance, formulation and  
180 dose) were evaluated using a stepwise inclusion ( $p < 0.05$ ) and elimination ( $p > 0.01$ ) approach,  
181 with linear functions for the continuous variables (namely, age, creatinine clearance and  
182 dose; centered on the median value). Creatinine clearance was calculated using the Chronic  
183 Kidney Disease Epidemiology Collaboration equation (23). We also considered estimating an  
184 interaction between the mean transit time and whether the dose contained split tablets (25  
185 mg dose only) or not.  
186  
187 Model discrimination was performed by assessing changes in the objective function value  
188 ( $\Delta\text{OFV}$ , calculated as proportional to minus twice the log-likelihood of data) and associated  
189  $\chi^2$  tests. Goodness of fit was assessed by inspection of diagnostic plots with consideration of  
190 parameter estimate (eta) shrinkage and epsilon shrinkage (24). A prediction-corrected visual  
191 predictive check (VPC) was performed for the final model ( $n=1000$ , stratified on metabolite).  
192 DBS samples from study 1 were omitted from the VPC due to the 10-fold different LLOQ. The  
193 VPC was visualized by plotting the 5<sup>th</sup>, 50<sup>th</sup> and 95<sup>th</sup> percentiles of the observed data overlaid

with the 95% confidence intervals of the same percentiles of the simulated data. The simulated and observed fraction of data below the limit of quantification were also visualized to evaluate the impact of data censoring. For the final model, relative standard errors and the 95% confidence intervals of parameter estimates were derived by bootstrap diagnostics stratified by formulation (104 replications only due to long run times).

Individually-estimated secondary PK parameters, including maximum concentration (C<sub>max</sub>), time to maximum concentration (T<sub>max</sub>), half-life and area under the concentration-time curve from time zero to 72 hours post-dose (AUC), were derived directly from NONMEM for each metabolite. In addition, a regression analysis of the terminal phase of model-predicted individual concentration-time profiles was performed to obtain estimates of half-life.

*O. viverrini* egg burdens expressed as eggs per gram of stool (epg) were determined as the mean of the four counts (or as many as were available) from the two slides of the two stool samples. The relative reduction in egg burden was calculated for each participant as  $100 \times (\text{burden at enrolment} - \text{burden at 21 days}) / (\text{burden at enrolment})$ . Cure was defined as no eggs detected at 21 days. Univariable logistic regression was used to assess the relationship between individually-estimated exposure parameters (i.e. C<sub>max</sub> and AUC) and cure.

## RESULTS

Overall, 68 participants were enrolled: 31 in the first study (13, 9 and 9 participants received 200, 400 and 600 mg, respectively) and 37 in the second study (9, 9, 9 and 10 participants received 25, 50, 100 and 200 mg, respectively). 35 (51%) participants were female, and the

median (interquartile range) age was 42 (31-48) years, weight 52 (47-57) kg, creatinine clearance 66 (50-112) mL/min per 1.73 m<sup>2</sup>, and *O. viverrini* egg burden 897 (435-1827) epg. A total of 1307 samples were analyzed for dADT (1303 for adADT), of which 300 were whole-blood, 669 plasma and 338 DBS. The mean number of whole-blood and plasma samples was ten per participant, and five for DBS (plus a baseline sample for each participant). Overall, 15 (5%) whole-blood, 81 (12%) plasma and 41 (12%) DBS dADT measurements were below the quantification limit; the corresponding figures for adADT were 38 (13%), 117 (18%) and 82 (24%), respectively.

#### **Structural model**

A one-compartment disposition model for each metabolite described the observed data well with no further improvement with additional distribution compartments. The transit-compartment absorption model was superior to a first-order absorption model, with an optimum number of 6 transit compartments. Adding proportional transformation factors for both plasma and DBS versus blood did not improve the model significantly, nor did incorporating inter-individual variability for the relative bioavailability, and therefore these models were not carried forward. Incorporating correlations between the clearance and volume parameters for both metabolites improved the model fit substantially ( $\Delta\text{OFV}=-28$ ), therefore this model was carried forward. Omitting concentrations quantified below the LLOQ resulted in model misspecification of the fraction of censored data (data not shown), which was described adequately using the M3 method, therefore the M3 method was used for the final model.

#### **Covariate modeling**

A number of parameter-covariate relationships were significant in the stepwise covariate approach. Compared to the 50 mg formulation used in study 2, the 200 mg formulation used in study 1 had 40.1% higher mean transit absorption time, 113% higher dADT volume of distribution, and 364% higher adADT volume of distribution. Each ten year increase in age was associated with 12.7% lower dADT clearance and 21.2% lower adADT clearance. The model incorporating an interaction between the mean transit time and whether the dose used split tablets (25 mg dose only) or not did not converge. The final model and parameter estimates are shown in Figure 1 and Table 1 (see Appendix for NONMEM code).

#### **Model diagnostics**

Goodness of fit diagnostics showed no obvious model misspecification but a small deviation at low concentrations was noted, likely due to censoring of data below the limit of quantification (Figure 2). For both metabolites, the population predictions tended to be underestimated for the lowest dose of 25 mg (Figures 2A and 2B, left panels). Eta and epsilon shrinkages were low ( $\leq 12\%$ ). The prediction-corrected visual predictive checks suggested reasonable model fit, albeit with some misspecification for the 95<sup>th</sup> percentiles at 24 hours and the 5<sup>th</sup> percentile for dADT (Figure 3).

#### **Secondary PK parameters and outcomes**

Model-derived estimates (i.e.  $\text{LN}(2) \times V_d/\text{CL}$ ) for the adADT elimination half-life were a factor of ten smaller than non-compartmental analysis (NCA) estimates (Duthaler *et al*, manuscript under review). A regression analysis of the terminal phase of model-predicted individual concentration-time profiles showed almost identical terminal elimination half-lives between the two metabolites (Table 2), indicating that the adADT metabolite is subject to formation-

rate limited elimination. Therefore, the half-lives determined by regression should be used for true representation of the elimination half-life, and are presented henceforth.

As expected, dADT and adADT estimated C<sub>max</sub>, AUC and elimination half-life typically increased with higher doses, suggesting dose-proportional pharmacokinetics (Table 2). There was large variability in the estimated T<sub>max</sub>, except for the 25 mg dose where split tablets were used and therefore the enteric coating of the tablet was destroyed.

Among 67 patients with results at 21 days, cure rates ranged between 11% (25 mg) and 100% (400 mg). The median (interquartile range; range) relative reductions in egg burden were 86% (60-92; 36-100), 93% (92-100; 83-100), 100% (99-100; 77-100), 100% (99-100; 63-100), 100% (100-100; 100-100), 100% (100-100; 91-100) for 25 mg, 50 mg, 100 mg, 200 mg, 400 mg, and 600 mg, respectively (Figure 4). Cure was associated with higher dADT C<sub>max</sub> and AUC ( $p=0.004$  and  $0.003$ , respectively). adADT exposure was not associated with cure ( $p\geq 0.15$ ).

## DISCUSSION

This first report on the population PK of tribendimidine, in persons infected with *O. viverrini*, supports the clinical development of tribendimidine for the treatment of liver fluke infections. We have shown that a central metabolite compartment model describes the PK of tribendimidine well, in agreement with previous analyses in healthy volunteers (10, 13, 15), with absorption captured by a flexible transit compartment model.

The availability of relatively large sample size and intensive sampling were key strengths of this analysis, which combined data across two similar studies and a broad range of doses. However, this added a complication to the analysis as there are known differences between the formulations of the tablets used in the two studies (200 mg tablets in the first study and 50 mg tablets in the second study), with 200 mg tablets being more likely to “float” *in vitro* and hence delay absorption (Duthaler *et al*, manuscript under review). These differences were captured by covariate modeling, with an interaction between formulation and mean transit absorption time (40% longer for the 200 mg tablets compared to the 50 mg tablets). Further, the modeling indicated that the volume of distribution for both dADT and adADT was higher with the 200 mg versus 50 mg formulation, but the reasons for this are not clear. However, the overall dADT exposure was similar between formulations and suggests that the effect of formulation might have limited clinical impact. Of note, the 200 mg tablet is that which is currently licensed for use in China. Besides formulation effects, interactions for age were incorporated in the model, with older age being associated with lower clearance for both metabolites, as might be expected (25). This could potentially result in under-exposure in younger patients after standard dosing, and further studies are warranted to address the dose-optimization in this group of patients.

A further strength of this study was the availability of drug concentrations measured in three biological fluids, namely whole-blood, plasma and DBS, and we were able to model these jointly, with no evidence of a difference between the fluids. Consistent with previous analyses (Duthaler *et al*, manuscript under review, and (16)), our findings support the use of the novel DBS methods for future PK studies, offering cheaper and more convenient sampling. The structural modeling applied in this study was used to inform the optimal

design of a population PK phase IIb study using DBS with sparse sampling. Based on previous analyses (Sayasone *et al*, manuscript under review), the phase IIb study used a dose of 400 mg, with 200 mg tablets. Subsequent work will aim to validate our model using the data from the phase IIb study.

We observed high correlation between clearance and volume of distribution for the each of the individual metabolites, as we might expect given that the treatment was administered orally. The inter-individual variability in relative bioavailability was close to zero, suggesting that potential between-patient variability was fully explained by the implemented variance-covariance matrix. We assumed a fixed renal clearance of dADT of 35%, based on a study from 2010 (10). An earlier study indicated that renal clearance may vary between 35-58%, but it was not possible to examine this analysis in detail (article in Chinese) (11). Urine data were not available for the presented study, so this could not be evaluated with the present data. The fixed renal clearance therefore simply acts as a scaling factor for the pharmacokinetic parameters.

Compared to a recent NCA of these data, our estimates of C<sub>max</sub> and AUC were broadly comparable for the metabolite adADT, but were somewhat lower for dADT (Table 3; Duthaler *et al*, manuscript under review). However, a NCA is highly dependent on the sampling design, and model-derived exposures might better correspond to the expected exposures. As discussed above, we observed that the metabolite adADT is subject to formation-rate limited elimination, and regression of the terminal phase of individual concentration-time data should be used to obtain a true representation of the half-life; our estimates were similar to those by NCA.

337

338 Previous PK studies of tribendimidine have only been conducted in healthy volunteers, who  
339 may be expected to have very different PK profiles (26). However, our estimates for C<sub>max</sub>  
340 and half-life were broadly comparable to those of previous studies, which also used one-  
341 compartment models (Table 3) (8, 13). Our estimated T<sub>max</sub> and AUC for dADT were typically  
342 higher than previously reported, but for adADT were comparable. We observed large  
343 variability in the estimated T<sub>max</sub>, except for the 25 mg dose where split tablets were used.  
344 Since the enteric coating had been destroyed for the 25 mg dosing, the absorption of the  
345 drug tended to be quicker and more consistent across patients. The long mean transit  
346 absorption time for dADT indicates slow absorption of the drug with prolonged residence in  
347 the stomach. For doses of at least 100 mg, 94% of estimated C<sub>max</sub> values were above the  
348 90% effective concentration (EC<sub>90</sub>) value of 75 ng/ml (as estimated by Duthaler *et al*,  
349 manuscript under review). Correspondingly, we observed relatively high cure rates of ≥55%  
350 with doses of at least 100 mg. There was a strong association between cure and both dADT  
351 C<sub>max</sub> and AUC. There was no evidence of an association between cure and adADT exposure,  
352 confirming the marginal activity of this metabolite.

353

354 In conclusion, we have described for the first time the structural population PK model for  
355 tribendimidine in *O. viverrini*-infected individuals. Our findings will contribute to informing  
356 the incorporation of tribendimidine into the suite of drugs available for the treatment and  
357 control of helminthic infections. Further PK/PD studies of tribendimidine are needed to  
358 validate the structural model, and confirm covariate relationships and associations between  
359 exposure parameters and cure.

360



361    **ACKNOWLEDGEMENTS**

362    We thank the participants of the study and staff at Champasack Provincial Hospital. This work  
363    was supported by the DFID/MRC/Wellcome Trust Joint Global Health Trials Scheme for  
364    financial support. The Wellcome Trust-Mahidol University-Oxford Tropical Medicine  
365    Research Programme is supported by the Wellcome Trust of Great Britain. We are grateful  
366    to Flavia Camponovo for her assistance in running the bootstraps.

367

368

## REFERENCES

1. **Sripa B, Kaewkes S, Intapan PM, Maleewong W, Brindley PJ.** Food-borne trematodiasis in Southeast Asia epidemiology, pathology, clinical manifestation and control. *Adv Parasitol* **72**:305–350.
2. **Van den Enden E.** Pharmacotherapy of helminth infection. *Expert Opin Pharmacother* **10**:435–451.
3. **Sayasone S, Odermatt P, Phoumindr N, Vongsaravane X, Sensombath V, Phetsouvanh R, Choulamany X, Strobel M.** Epidemiology of *Opisthorchis viverrini* in a rural district of southern Lao PDR. *Trans R Soc Trop Med Hyg* **101**:40–47.
4. **Keiser J, Utzinger J.** The drugs we have and the drugs we need against major helminth infections. *Adv Parasitol* **73**:197–230.
5. **Keiser J, Utzinger J.** Emerging foodborne trematodiasis. *Emerg Infect Dis* **11**:1507–1514.
6. **Panic G, Duthaler U, Speich B, Keiser J.** Repurposing drugs for the treatment and control of helminth infections. *Int J Parasitol Drugs Drug Resist* **4**:185–200.
7. **Xiao S-H, Hui-Ming W, Tanner M, Utzinger J, Chong W.** Tribendimidine: a promising, safe and broad-spectrum anthelmintic agent from China. *Acta Trop* **94**:1–14.
8. **Xiao S-H, Utzinger J, Tanner M, Keiser J, Xue J.** Advances with the Chinese anthelmintic drug tribendimidine in clinical trials and laboratory investigations. *Acta Trop* **126**:115–126.
9. **Soukhathammavong P, Odermatt P, Sayasone S, Vonghachack Y, Vounatsou P, Hatz C, Akkhavong K, Keiser J.** Efficacy and safety of mefloquine, artesunate, mefloquine-artesunate, tribendimidine, and praziquantel in patients with *Opisthorchis viverrini*: a randomised, exploratory, open-label, phase 2 trial. *Lancet Infect Dis* **11**:110–118.
10. **Yuan G, Xu J, Qu T, Wang B, Zhang R, Wei C, Guo R.** Metabolism and disposition of tribendimidine and its metabolites in healthy Chinese volunteers. *Drugs RD* **10**:83–90.
11. **Yuan G, Wei C, Wang B, Zhang R, Xu J, Guo R.** Metabolism and excretion of tribendimidine in healthy human volunteers. *Chin J New Drugs Clin Remedies* **27**:667–670.
12. **Xiao S, Xue J, Xu L, Zheng Q, Qiang H, Zhang Y.** The in vitro and in vivo effect of tribendimidine and its metabolites against *Clonorchis sinensis*. *Parasitol Res* **105**:1497–1507.
13. **Dou X, Yuan G, Zhang R, Wei C, Wang B, Guo R.** Pharmacokinetic study of dADT and acetylated dADT, metabolites of tribendimidine in human. *J Pharm Res* **32**:543–545.
14. **Xu J, Yuan G, Wei C, Wang B, Guo R.** Determination of urinary tribendimidine metabolite-terephthalic acid by HPLC. *J Shandong Univ Health Sci* **46**:1016–1019.
15. **Yuan G, Wang B, Wei C, Zhang R, Guo R.** LC–MS determination of p-(1-dimethylamino ethylimino)aniline: a metabolite of tribendimidine in human plasma. *Chromatographia* **68**:139–142.
16. **Duthaler U, Keiser J, Huwyler J.** LC-MS/MS method for the determination of two metabolites of tribendimidine, deacylated amidantel and its acetylated metabolite in plasma, blood and dried blood spots. *J Pharm Biomed Anal* **105**:163–173.

- 407 17. **Beal S, Sheiner L, Boeckman A, Bauer R.** NONMEM users' guides (1989-2009).
- 408 18. Pirana Software and Consulting. <http://www.pirana-software.com/> Accessed April 16, 2014.
- 409 19. **Lindbom L, Ribbing J, Jonsson EN.** Accessed April 22, 2014. Perl-speaks-NONMEM (PsN)—a Perl  
410 module for NONMEM related programming. *Comput Methods Programs Biomed* **75**:85–94.
- 411 20. **Tarning J, Thana P, Phyo AP, Lwin KM, Hanpithakpong W, Ashley EA, Day NPJ, Nosten F, White**  
412 **NJ.** Population pharmacokinetics and antimalarial pharmacodynamics of piperazine in patients  
413 with plasmodium vivax malaria in Thailand. *CPT Pharmacomet Syst Pharmacol* **3**:e132.
- 414 21. **Beal SL.** Ways to fit a PK model with some data below the quantification limit. *J Pharmacokinet*  
415 *Pharmacodyn* **28**:481–504.
- 416 22. **Holford NH.** A size standard for pharmacokinetics. *Clin Pharmacokinet* **30**:329–332.
- 417 23. **Levey AS, Stevens LA, Schmid CH, Zhang YL, Castro AF 3rd, Feldman HI, Kusek JW, Eggers P, Van**  
418 **Lente F, Greene T, Coresh J.** A new equation to estimate glomerular filtration rate. *Ann Intern*  
419 *Med* **150**:604–612.
- 420 24. **Savic RM, Karlsson MO.** Importance of shrinkage in empirical Bayes estimates for diagnostics:  
421 Problems and solutions. *AAPS J* **11**:558–569.
- 422 25. **Greenblatt D, Koch-Weser J, Sellers EM, Shader RI.** Drug disposition in old age. *N Engl J Med*  
423 **306**:1081–1088.
- 424 26. **Na Bangchang K, Karbwang J, Pungpak S, Radomyos B, Bunnag D.** Pharmacokinetics of  
425 praziquantel in patients with opisthorchiasis. *Southeast Asian J Trop Med Public Health* **24**:717–  
426 723.

427

428

## TABLES

**Table 1. Population pharmacokinetic parameter estimates from the final model describing tribendimidine metabolites in adults with *Opisthorchis viverrini*.**

	Population estimate [1]	95% confidence interval [2]	Relative standard error [2]
Transit compartments	6 ( <i>fixed</i> )	-	-
Mean transit time, hour	3.38	2.51, 4.63	14.5
Metabolite dADT			
$CL/F$ , L/h	16.7	14.6, 18.1	5.12
$V_C/F$ , L	93.3	74.3, 112	8.49
$\sigma$ (% CV) [3]	116%	94.1, 141%	12.6
Metabolite adADT			
$CL/F$ , L/h	41.8	31.9, 55.2	13.5
$V_C/F$ , L	11.5	6.78, 20.3	25.0
$\sigma$ (% CV) [3]	63.9%	50.1, 77.3%	15.6
Covariate effects (%)			
Formulation on mean transit time [4]	40.1%	2.96, 96.9%	48.7
Formulation on dADT $V_C/F$ [4]	113%	53.0, 196%	31.6
Formulation on adADT $V_C/F$ [4]	364%	141, 499%	29.0
Age on dADT $CL/F$ , per 10 years older	-12.7%	-19.9, -8.08%	22.5
Age on adADT $CL/F$ , per 10 years older	-21.2%	-42.1, -3.72%	43.4
Inter-individual variability (% CV) [3]			
Mean transit time	88.5%	72.0, 111%	16.9
dADT $CL/F$	24.8%	14.1, 34.6%	34.9
dADT $V_C/F$	101%	62.5, 141%	29.5
adADT $CL/F$	106%	81.5, 150%	19.8
adADT $V_C/F$	134%	82.9, 258%	33.6
Correlations (% CV) [5]			
dADT $CL/F$ and dADT $V_C/F$	91.8%	74.8, 98.9%	26.6
dADT $CL/F$ and adADT $CL/F$	-62.6%	-92.9, -20.1%	38.5
dADT $CL/F$ and adADT $V_C/F$	15.2%	-49.6, 59.2%	126
dADT $V_C/F$ and adADT $CL/F$	-46.1%	-72.4, -9.37%	53.3
dADT $V_C/F$ and adADT $V_C/F$	51.8%	-9.50, 72.8%	37.3
adADT $CL/F$ and adADT $V_C/F$	34.0%	-8.01, 68.9%	54.3

$CL$ , clearance;  $F$ , bioavailability;  $V_C$ , apparent central volume of distribution;  $\sigma$ , additive residual error; CV, coefficient of variation. Results shown are for a typical patient aged 52 years, weighing 51.5 kg and receiving 50 mg tablets (study 2). [1] Population estimates are from NONMEM. [2] Confidence intervals and relative standard errors are estimated by bootstrap (104 replications). [3] Calculated as  $\sqrt{(\exp(\eta_\theta) - 1)} \times 100$ . [4] 200 mg tablets (study 1) versus 50 mg tablets (study 2). [5] Calculated as  $correlation\ estimate / \sqrt{(\eta_{\theta 1} \times \eta_{\theta 2})} \times 100$ .

**Table 2. Secondary pharmacokinetic parameter estimates from the final population pharmacokinetic model.**

Dose, mg	Cmax, ng/mL	Tmax, h	Half-life, h [1]	AUC, h×ng/mL
<b>Metabolite dADT</b>				
25	67 (61-70)	1.75 (1.56-2.21)	4.67 (3.70-5.00)	488 (448-515)
50	105 (71-115)	12.20 (6.07-14.10)	2.81 (2.26-3.58)	957 (857-1099)
100	246 (201-275)	5.99 (3.92-8.16)	3.30 (2.51-3.67)	2275 (1798-2491)
200	414 (341-511)	7.76 (5.54-9.31)	4.09 (3.17-4.61)	3924 (3459-5327)
400	821 (317-873)	7.07 (4.21-8.48)	4.83 (4.36-12.41)	7798 (6653-10219)
600	953 (440-1058)	6.54 (4.97-8.52)	5.00 (4.24-10.64)	10831 (8162-14584)
<b>Metabolite adADT</b>				
25	25 (5-34)	2.28 (2.06-2.43)	4.67 (3.70-5.00)	161 (44-235)
50	18 (16-42)	12.20 (6.18-14.20)	2.81 (2.26-3.58)	363 (199-398)
100	101 (91-109)	6.12 (4.42-8.47)	3.30 (2.51-3.67)	809 (690-1013)
200	60 (38-237)	8.51 (6.04-9.79)	4.09 (3.17-4.61)	972 (436-2399)
400	116 (69-202)	9.22 (7.96-11.20)	4.83 (4.36-12.41)	2049 (878-4975)
600	235 (215-387)	8.89 (5.52-11.90)	5.00 (4.24-10.63)	4033 (2958-6050)

Cmax, maximum concentration; Tmax, time to reach maximum concentration; AUC, area under the concentration-time curve (0-72 hours). Results are presented as median (interquartile range). [1] Estimated by regression analysis of the terminal phase of model-predicted individual concentration-time profiles.

445 **Table 3. Comparison of our compartmental model results with NCA analysis and the literature.**

Source	Participants	N	Cmax, ng/mL	Tmax, h	Half-life, h [1]	AUC, h×ng/mL [2]
<b>Metabolite dADT</b>						
<b>Dose 25 mg</b>						
Compartmental model results	<i>O. viverrini</i> infection	9	67 (61-70)	1.75 (1.56-2.21)	4.67 (3.70-5.00)	488 (448-515)
NCA results [3]	<i>O. viverrini</i> infection	9	68 (62-88)	3 (3-4)	4 (4-5) [4]	485 (410-535) [5]
<b>Dose 50 mg</b>						
Compartmental model results	<i>O. viverrini</i> infection	9	105 (71-115)	12.20 (6.07-14.10)	2.81 (2.26-3.58)	957 (857-1099)
NCA results [3]	<i>O. viverrini</i> infection	9	252 (230-327)	6 (4-8)	3 (3-4) [4]	1712 (1486-2091) [5]
<b>Dose 100 mg</b>						
Compartmental model results	<i>O. viverrini</i> infection	9	246 (201-275)	5.99 (3.92-8.16)	3.30 (2.51-3.67)	2275 (1798-2491)
NCA results [3]	<i>O. viverrini</i> infection	9	508 (372-566)	4 (3-5)	4 (3-5) [4]	2768 (2111-3170) [5]
<b>Dose 200 mg</b>						
Compartmental model results	<i>O. viverrini</i> infection	23	414 (341-511)	7.76 (5.54-9.31)	4.09 (3.17-4.61)	3924 (3459-5327)
NCA results for 4x50 mg [3]	<i>O. viverrini</i> infection	9	701 (543-789)	4 (3-5)	4 (4-5) [4]	5008 (4222-6138) [5]
NCA results for 1x200 mg [3]	<i>O. viverrini</i> infection	13	744 (562-1098)	5 (4-8)	4 (3-5) [4]	6460 (5659-7802) [5]
Yuan <i>et al</i> 2008 (15) [6]	Healthy volunteers	12	370	3.60	4.25	2120
<b>Dose 400 mg</b>						
Compartmental model results	<i>O. viverrini</i> infection	9	821 (317-873)	7.07 (4.21-8.48)	4.83 (4.36-12.41)	7798 (6653-10219)
NCA results [3]	<i>O. viverrini</i> infection	9	1398 (1254-1558)	8 (6-10)	4 (4-5) [4]	12044 (11055-13916) [5]
Yuan <i>et al</i> 2008 (15) [6]	Healthy volunteers	12	640	4.20	4.74	4450
Dou <i>et al</i> 2013 (13) [6]	Healthy volunteers	8	449	5.25	5.38	4769
<b>Dose 600 mg</b>						
Compartmental model results	<i>O. viverrini</i> infection	9	953 (440-1058)	6.54 (4.97-8.52)	5.00 (4.24-10.64)	10831 (8162-14584)
NCA results [3]	<i>O. viverrini</i> infection	9	1351 (1294-1561)	6 (4-8)	4 (4-5) [4]	14003 (12309-15555) [5]
Yuan <i>et al</i> 2008 (15) [6]	Healthy volunteers	12	890	3.60	5.69	7660
<b>Metabolite adADT</b>						
<b>Dose 25 mg</b>						

Source	Participants	N	Cmax, ng/mL	Tmax, h	Half-life, h [1]	AUC, h×ng/mL [2]
Compartmental model results	<i>O. viverrini</i> infection	9	25 (5-34)	2.28 (2.06-2.43)	4.67 (3.70-5.00)	161 (44-235)
NCA results [3]	<i>O. viverrini</i> infection	9	26 (6-29)	4 (3-4)	5 (4-6) [4]	165 (48-239) [5]
Dose 50 mg						
Compartmental model results	<i>O. viverrini</i> infection	9	18 (16-42)	12.20 (6.18-14.20)	2.81 (2.26-3.58)	363 (199-398)
NCA results [3]	<i>O. viverrini</i> infection	9	53 (13-82)	6 (4-8)	4 (4-5) [4]	537 (235-708) [5]
Dose 100 mg						
Compartmental model results	<i>O. viverrini</i> infection	9	101 (91-109)	6.12 (4.42-8.47)	3.30 (2.51-3.67)	809 (690-1013)
NCA results [3]	<i>O. viverrini</i> infection	9	117 (88-180)	5 (3-6)	4 (4-5) [4]	816 (764-1142) [5]
Dose 200 mg						
Compartmental model results	<i>O. viverrini</i> infection	23	60 (38-237)	8.51 (6.04-9.79)	4.09 (3.17-4.61)	972 (436-2399)
NCA results for 4x50 mg [3]	<i>O. viverrini</i> infection	10	144 (46-243)	5 (4-7)	4 (4-5) [4]	2114 (1572-2468) [5]
NCA results for 1x200 mg [3]	<i>O. viverrini</i> infection	13	45 (34-142)	8 (6-10)	6 (5-8) [4]	574 (506-1399) [5]
Dose 400 mg						
Compartmental model results	<i>O. viverrini</i> infection	9	116 (69-202)	9.22 (7.96-11.20)	4.83 (4.36-12.41)	2049 (878-4975)
NCA results [3]	<i>O. viverrini</i> infection	9	216 (56-398)	10 (8-10)	6 (5-7) [4]	1654 (920-2854) [5]
Dou <i>et al</i> 2013 (13) [6]	Healthy volunteers	8	148	7.13	7.09	1989
Dose 600 mg						
Compartmental model results	<i>O. viverrini</i> infection	9	235 (215-387)	8.89 (5.52-11.90)	5.00 (4.24-10.63)	4033 (2958-6050)
NCA results [3]	<i>O. viverrini</i> infection	9	345 (200-427)	8 (6-10)	6 (6-6) [4]	3601 (2457-4571) [5]

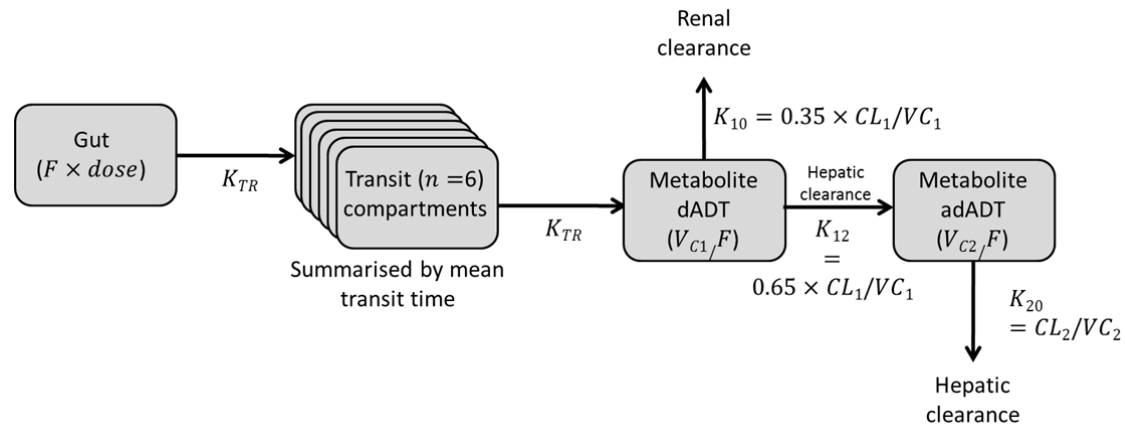
446 Cmax, maximum concentration; Tmax, time to reach maximum concentration; AUC, area under the concentration-time curve; NCA, non-compartmental analysis (performed  
447 using WinNonLin version 5.2 (Pharsight Corporation, USA)). Results are presented as median (interquartile range) where available; it is not clear whether the results reported in  
448 Yuan *et al* (15) and Dou *et al* (13) are medians or means. [1] Estimated by regression analysis of the terminal phase of model-predicted individual concentration-time profiles.  
449 [2] AUC 0-72 hours for the compartmental model results and otherwise AUC 0-infinity. [3] Duthaler *et al*, manuscript under review. Plasma results shown, which are a subset of  
450 the data used in this study. [4] Calculated where possible using half-life=LN(2)/λ where the elimination rate constant λ was determined by linear regression of the LN-

451 transformed concentration values in the elimination phase. [5] Calculated where possible using the trapezoidal rule of the LN-concentration by time profile. [6] One-  
452 compartment model.



## FIGURES

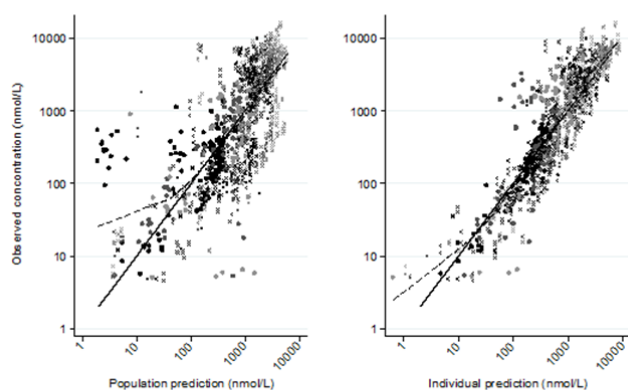
**Figure 1. Final structural pharmacokinetic model for tribendimidine metabolites in adults with *Opisthorchis viverrini*.**



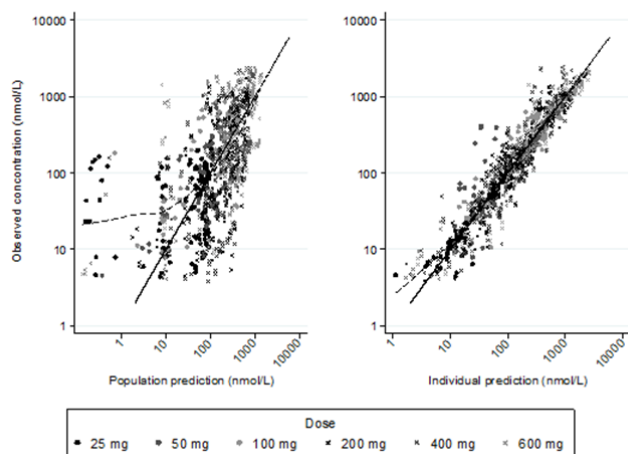
Model is a six-transit absorption model with a one-compartment disposition model for each metabolite dADT and adADT.  $F$ , bioavailability;  $K_{TR}$ , transit absorption rate;  $n$ , total number of compartments (mean transit time  $= (n + 1)/K_{TR}$ );  $CL$ , clearance;  $V_C$ , apparent central volume of distribution (subscript 1 for dADT and subscript 2 for adADT).

464 **Figure 2. Goodness-of-fit diagnostics for the final pharmacokinetic model.**

**A. dADT**



**B. adADT**



465

466 From left to right, plots show: observed versus population predicted concentrations; observed versus individual

467 predicted concentrations. Data points are shown by dose. Solid lines show the line of identity; dashed lines

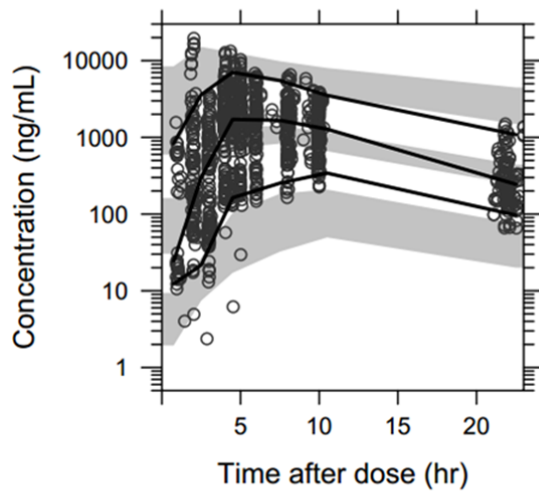
468 show a locally-weighted regression line.

469

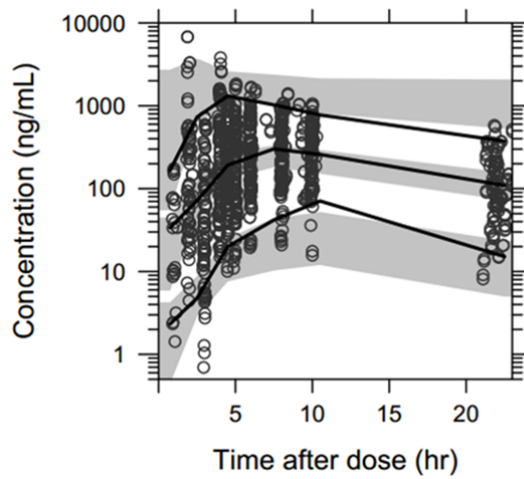
470

**Figure 3. Visual predictive checks of the final pharmacokinetic model.**

**A. dADT.**

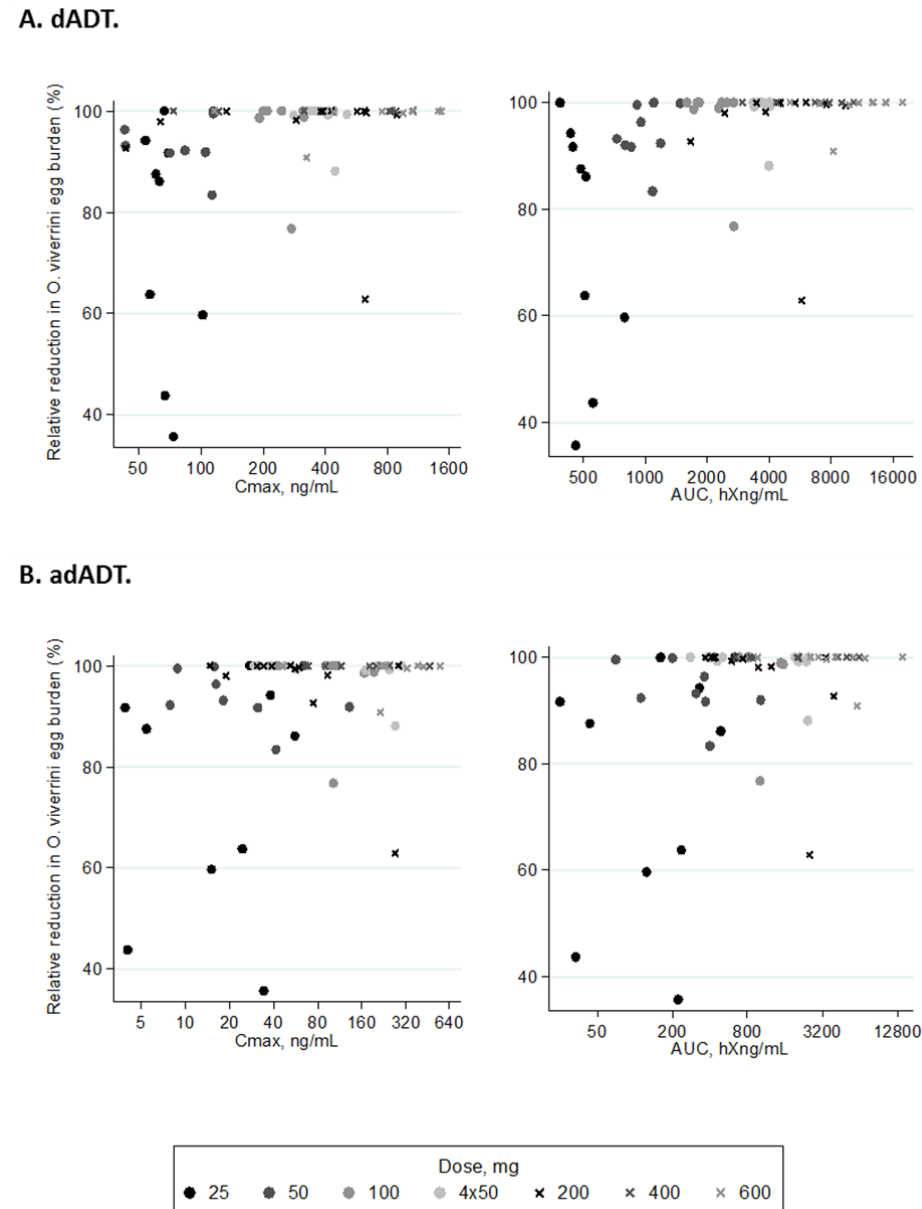


**B. adADT.**

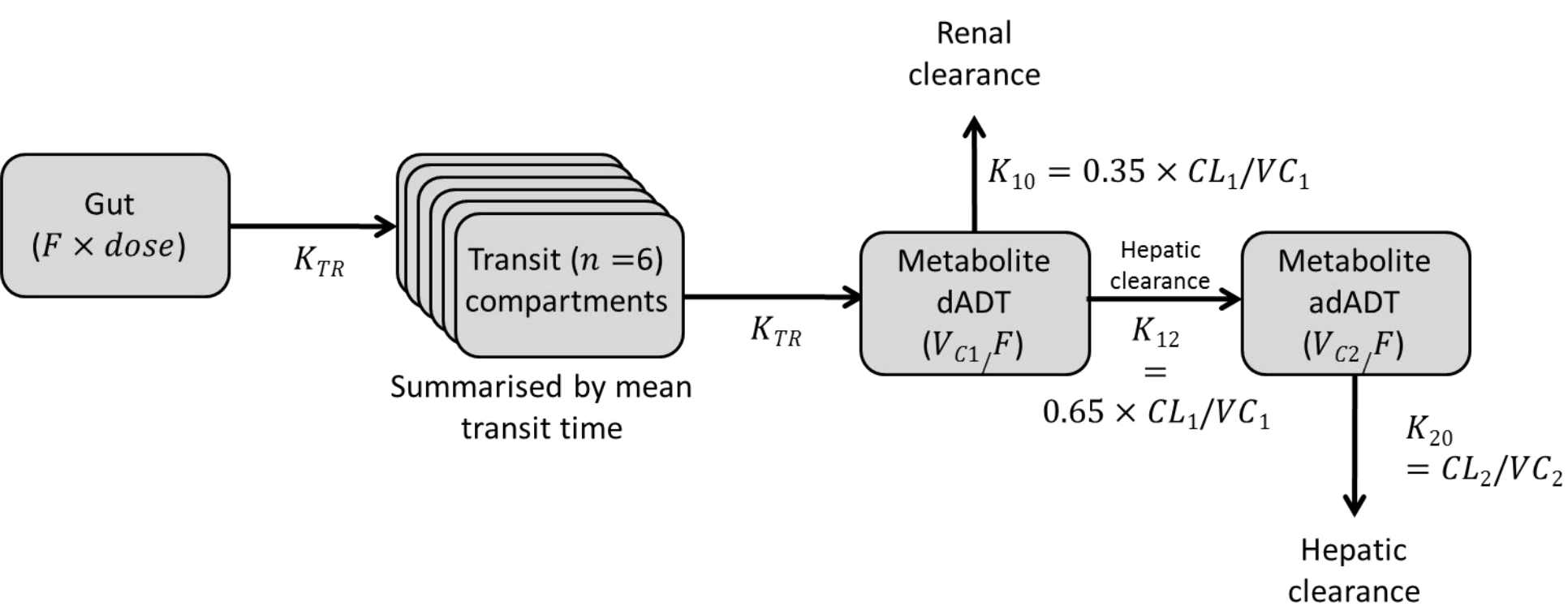


Visual predictive checks illustrating concentration of metabolite (**A** dADT, **B** adADT) versus time. Open circles indicate the observed data, black lines indicate the 5<sup>th</sup>, 50<sup>th</sup> and 95<sup>th</sup> percentiles of the observed data, and the grey bands indicate the 95% confidence intervals of the same percentiles of the simulated data. Results exclude DBS from study 1 due to the 10-fold different limit of quantification.

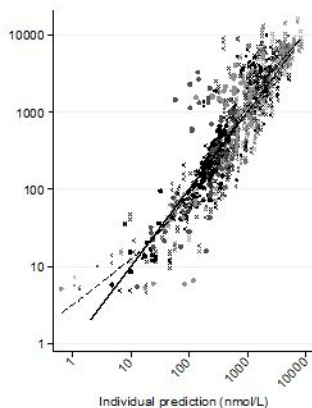
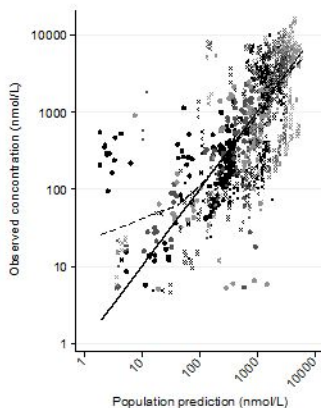
**Figure 4. Relative reduction in *O. viverrini* egg burden by exposure parameters.**



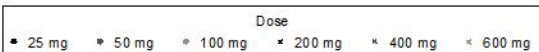
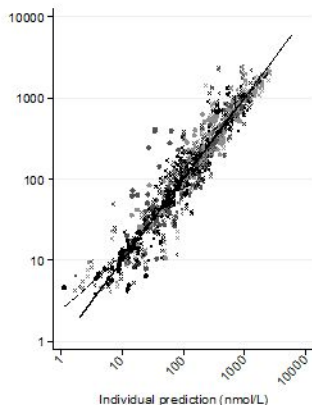
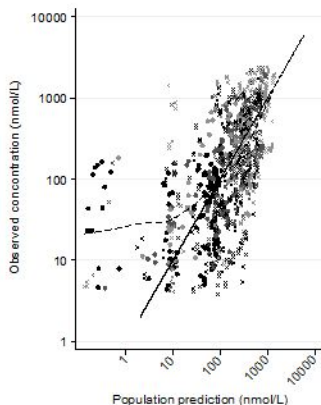
Observed relative reduction in *O. viverrini* egg burden from baseline to 21 days later versus estimated exposure parameters (Cmax and AUC) for each patient, where 100% relative reduction indicates cure (**A**: results for metabolite dADT and **B**: results for metabolite adADT). Doses of 25, 50, 100 and 4x50 mg using 50 mg tablets in study 2 are indicated by filled circles with darker colors for lower doses; doses of 200, 400 and 600 mg using 200 mg tablets in study 1 are indicated by crosses with darker colors for lower doses. Cmax, maximum concentration; AUC, area under the concentration-time curve (0-72 hours).



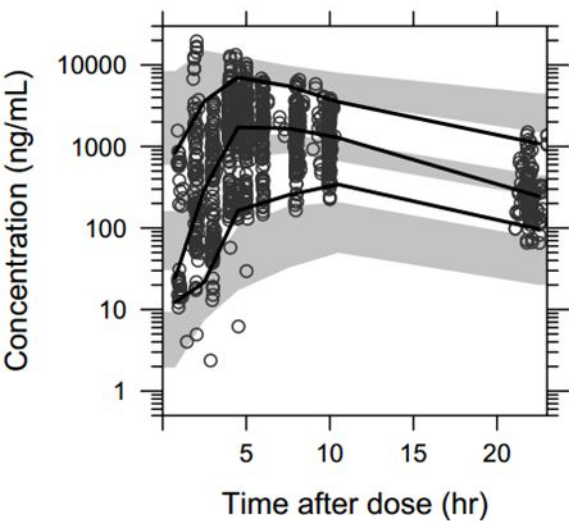
## A. dADT



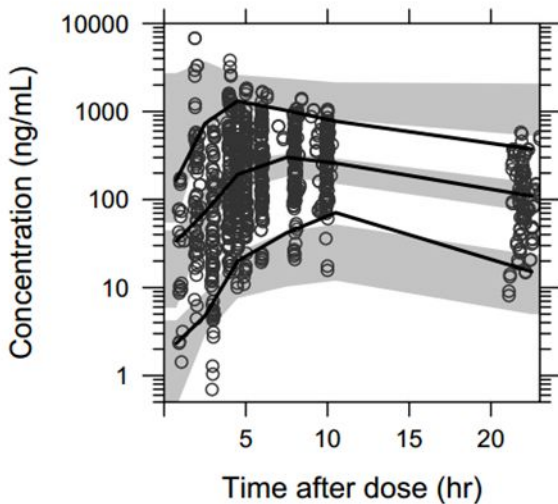
## B. adADT



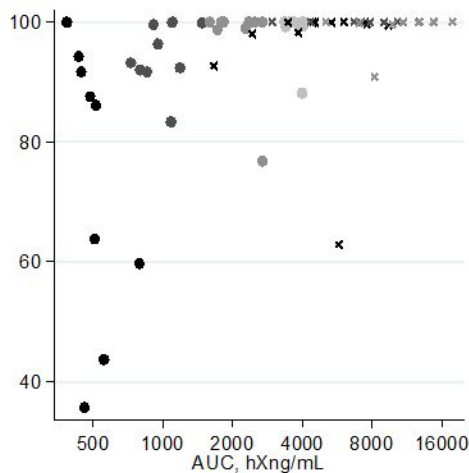
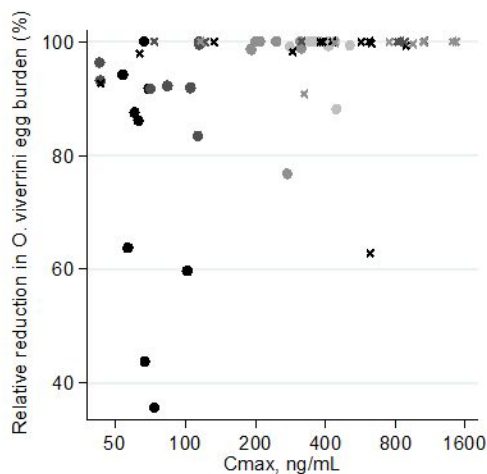
## A. dADT.



## B. adADT.



## A. adADT.



## B. adADT.

